# Communications Research Centre

## A STRUCTURAL DYNAMICS MODEL FOR FLEXIBLE SOLAR ARRAYS OF THE COMMUNICATIONS TECHNOLOGY SATELLITE

by

F. VIGNERON



CRC REPORT NO. 1268

Department of Communications
Ministère des Communications



OTTAWA, APRIL 1975

COMMUNICATIONS RESEARCH CENTRE

DEPARTMENT OF COMMUNICATIONS
CANADA



# A STRUCTURAL DYNAMICS MODEL FOR FLEXIBLE SOLAR ARRAYS OF THE COMMUNICATIONS TECHNOLOGY SATELLITE

by

F. Vigneron

*(Space Technology Branch)*



CRC REPORT NO. 1268

*April 1975*
OTTAWA

TABLE OF CONTENTS

NOMENCLATURE . . . . . v

ABSTRACT . . . . . 1

1. INTRODUCTION . . . . . 2

2. MODELING OF COMPONENTS . . . . . 2

2.1 Boom . . . . . 2
2.2 Blanket . . . . . 5
2.3 Inboard Pallet and Elevator Arms . . . . . 6
2.4 Tip Pallet . . . . . 6
2.5 Array Tensioning Spring . . . . . 7
2.6 Torsion Control Device . . . . . 7

3. CONFIGURATION AND METHOD OF GROUND TEST . . . . . 8

4. POTENTIAL ENERGY, KINETIC ENERGY, AND CONSTRAINT EQUATIONS . . . . . 8

4.1 Constraints Among Variables . . . . . 8
4.2 Potential Energy . . . . . 11
4.3 Kinetic Energy . . . . . 12

5. DISCRETIZATION . . . . . 13

5.1 Series Expansions and Discrete Variables . . . . . 13
5.2 Potential Energy . . . . . 14
5.3 Kinetic Energy . . . . . 15
5.4 Constraint Relations . . . . . 17

6. EQUATIONS OF STATIC EQUILIBRIUM AND MOTION . . . . . 18

7. APPLICATION IN CTS PROGRAM . . . . . 19

7.1 Calculated Frequencies and Mode Shapes . . . . . 19
7.2 Comparison of Numerical Results with Test Data . . . . . 20
7.3 Remarks on Prediction of On-Orbit Array Characteristics . . . . 26
7.4 Comments on Analyses of Refs. 4 - 7 . . . . . 27

8. CONCLUDING REMARKS . . . . . 27
9. ACKNOWLEDGMENTS . . . . . 27
10. REFERENCES . . . . . 28

## NOMENCLATURE

| | |
|---|---|
| $a$ | distance from boom centerline to pallet center of mass |
| $b,b'$ | width, and 'effective width', of blanket |
| $B^p$ | functional defined in Eq. (33) |
| $e$ | distance from boom centerline to blanket centerline |
| $EI_1$, $EI_2$ | bending stiffness' of the boom |
| $f_o$ | torsion control line force (one line) |
| $F$ | column matrix of applied force components |
| $f_a$ | force associated with array tensioning spring assembly |
| $g$ | gravitational constant (32.2 ft/sec$^2$) |
| $G$ | matrix of solar array internal forces, Eq. (36) |
| $H^p$ | functional defined in Eq. (34) |
| $k_{r1}$ | boom root stiffness, out-of-plane |
| $k_{r2}$ | boom root stiffness, in-plane |
| $h$ | $\ell_1 - \ell_2$ (Figure 1) |
| $I_z$ | moment of inertia of blanket, inboard pallet, and tip pallet, about Oz axis |
| $I_{px}, I_{py}, I_{pz}$ | moments of inertia of the tip pallet about the pallet center of mass |
| $JG$ | torsional stiffness constant of boom |
| $J^p$ | functional defined in Eq. (35) |
| $k_3$ | spring constant at blanket-tip pallet connection |

| | |
|---|---|
| $k_2$ | equivalent spring constant of the inboard pallet and elevator arm assembly |
| K | stiffness matrix relating to solar array, Eq. (32) |
| $\ell_1$ | length of boom |
| $\ell_2$ | length of blanket |
| $m_1$ | mass of tip pallet |
| $m_2$ | mass of the inboard pallet |
| M | mass matrix of array, Eq. (39) |
| $N_u, N_v, N_\zeta, N_\alpha$ | order of series expansions, Eqs. (25a) - (25d) |
| N | $(N_u+N_v+N_\zeta+N_\alpha-2)$, the order of discretization of the total structure |
| Oxyz<br>O'x'y'z' | reference frames associated with the solar array (Figure 1) |
| $p(\xi)$ | column matrix of functions |
| q | variable describing motion about equilibrium shape, Eq. (50) |
| $q_n$ | variable describing characteristic mode shapes of solar array, Eq. (54) |
| $Q^p$ | functional defined in Eq. (42) |
| t | time |
| $T_o$ | net blanket tension |
| u(x,t) | out-of-plane deformation function for boom (Figure 2) |
| $u_1(t)$, etc. | time varying elements of series expansion for u(x,t) |
| $\bar{u}$ | matrix, Eq. (26) |

| | |
|---|---|
| $\bar{U}(t)$ | forcing function for out-of-plane excitation |
| $v(x,t)$ | in-plane deformation function for boom (Figure 2) |
| $\bar{v}_1(t)$, etc. | time varying elements of series expansion for $v(x,t)$ |
| $\bar{v}$ | matrix, Eq. (25) |
| $V(t)$ | forcing function for in-plane excitation |
| $V$ | potential energy of solar array |
| $w(x'y',t)$ | deflection of the blanket, out-of-plane |
| $Z$ | defined in Eq. (29) |
| $z$ | defined in Eq. (44) |
| $z_o$ | matrix relating to static equilibrium shape (Eq. 52) |
| $\alpha(x,t)$ | torsional deformation of blanket about its centerline (Figure 3) |
| $\bar{\alpha}_1(t)$, etc. | time varying elements of series expansion for $\alpha(x',t)$ |
| $\bar{\alpha}$ | Matrix, Eq. (25) |
| $\beta(t)$ | angular in-plane rotation of blanket about parking spring pivotal point (Figure 3) |
| $\epsilon_b(x',y',t)$ | deformation of the blanket in the Ox direction |
| $\epsilon_T$ | extension of torsion control device |
| $\epsilon$ | extension of array tensioning spring |
| $\zeta(x',t)$ | out-of-plane deformation of blanket centerline (Figure 3) |
| $\bar{\zeta}_1(t)$, etc. | time varying elements of series expansion for $\zeta(x',t)$ |
| $\bar{\zeta}$ | matrix, Eq. (25) |
| $\bar{\bar{\zeta}}$ | defined in Eq. (45) |

| | |
|---|---|
| $\zeta_k^*$ | damping coefficient of the kth mode |
| $\eta_k(t)$ | modal coordinate function for the kth mode |
| $\Lambda(\xi), \Lambda_1(\xi)$, etc. | spatial deformation functions, Eqs. (25), (27) |
| $\nu(\xi), \nu_1(\xi)$, etc. | spatial deformation functions, Eqs. (23), (27) |
| $\chi(t)$ | motion of base of elevator arm assembly in Oy direction |
| $\xi$ | dummy integration variable, $x/\ell_1$, $x'/\ell_2$ |
| $\Xi^p$ | functional defined in Eq. (41) |
| $\Pi$ | constant matrix, Eq. (46) |
| $\rho_1$ | mass per foot of boom |
| $\rho_2$ | mass per foot of blanket |
| $\sigma$ | twist angle of boom tip |
| $\sigma_o(t)$ | forcing function for torsional excitation |
| $\Phi, \Phi_1(\xi)$, etc. | spatial deformation function sets, Eqs. (27), (29) |
| $\Psi, \Psi_1(\xi)$, etc. | spatial deformation function sets, Eq. (29) |
| $\overline{\overline{\Psi}}(\xi)$ | defined in Eq. (47) |
| $\omega_n$ | characteristic frequencies of solar array, Eq. (54) |

# A STRUCTURAL DYNAMICS MODEL FOR FLEXIBLE SOLAR ARRAYS OF THE COMMUNICATIONS TECHNOLOGY SATELLITE

by

F. Vigneron

ABSTRACT

A mathematical model, which describes the structural mechanics of flexible solar arrays of the Communications Technology Satellite (CTS) in a ground test configuration, is developed using variational principles and continuum mechanics methods. Modes and frequencies for an array with CTS parameters are calculated for the one-g test state, and compared to corresponding ones for the zero-g on-orbit state. Calculated results are compared with ground test data; good agreement is noted for the major structural frequencies and modes. The model does not predict certain observed higher frequency membrane-like blanket modes attributable to non-uniform tension distribution in the solar array blanket. Also the test results show that modal frequencies may be excited by subharmonic excitation; this feature would necessitate a non-linear vibrational model, and is not accounted for in the mathematical model. Alternate mathematical models based on finite element and continuum mechanics methods, which were developed for the design phase of the CTS program, are discussed in the light of test data and modeling of this report.

# 1. INTRODUCTION

This report presents a mathematical model of the structural mechanics of the solar arrays of the Communications Technology Satellite (CTS)[1]. The model describes the behaviour of an array in its fully deployed state, with particular attention given to vibrational excitation in ground test configuration (i.e., under one-g environment, in vacuum).

The modeling was originally developed in January, 1973, about six months prior to solar array testing in CRC's 10' x 30' vacuum chamber facility[2,3], and the results served as a guide for planning the test work. Subsequent to the testing, modifications were made in the original modeling to reflect certain minor mechanisms and interactions which came to light during testing.

The modeling presented herein thus incorporates the knowledge gained in testing. It adequately describes the major structural mechanics features observed in the ground testing. Minor shortcomings of the modeling are noted and discussed. Structural dynamics models of the CTS array which were derived during the design phase of the CTS program in the period 1970 - 72[4-7] are also discussed.

# 2. MODELING OF COMPONENTS

The CTS deployable solar array, a fold-up flat-pack type, is designed to be stowed during the spacecraft launch phase and deployed while the spacecraft is in orbit[1]. The array in its deployed state is, from an analysis point of view, composed of six subcomponents depicted in Figure 1: the boom and actuator, the blanket, the inboard pallet and elevator arms, the tip pallet, the array tensioning spring, and the torsion control lines. The boom and actuator provides the basic energy and force for the deployment process, and induces a final tensioned state. The total assemblage is described herein with respect to coordinate systems Oxyz and O'x'y'z', also depicted in Figure 1. The parameters associated with solar arrays of the CTS Program are listed in Table 1.

## 2.1 BOOM

The boom is modeled as a beam with elastic properties conforming to those expressed through the potential,

$$\frac{1}{2}\int_0^{\ell_1} (EI_1\, u_{xx}^2 + EI_2\, v_{xx}^2)\, dx + \frac{1}{2}\, JG\, (\sigma - \sigma_o)^2/\ell_1 \qquad (1)$$

The coordinates of the boom are depicted in Figure 2. It is assumed that the boom centerline is inextensible.

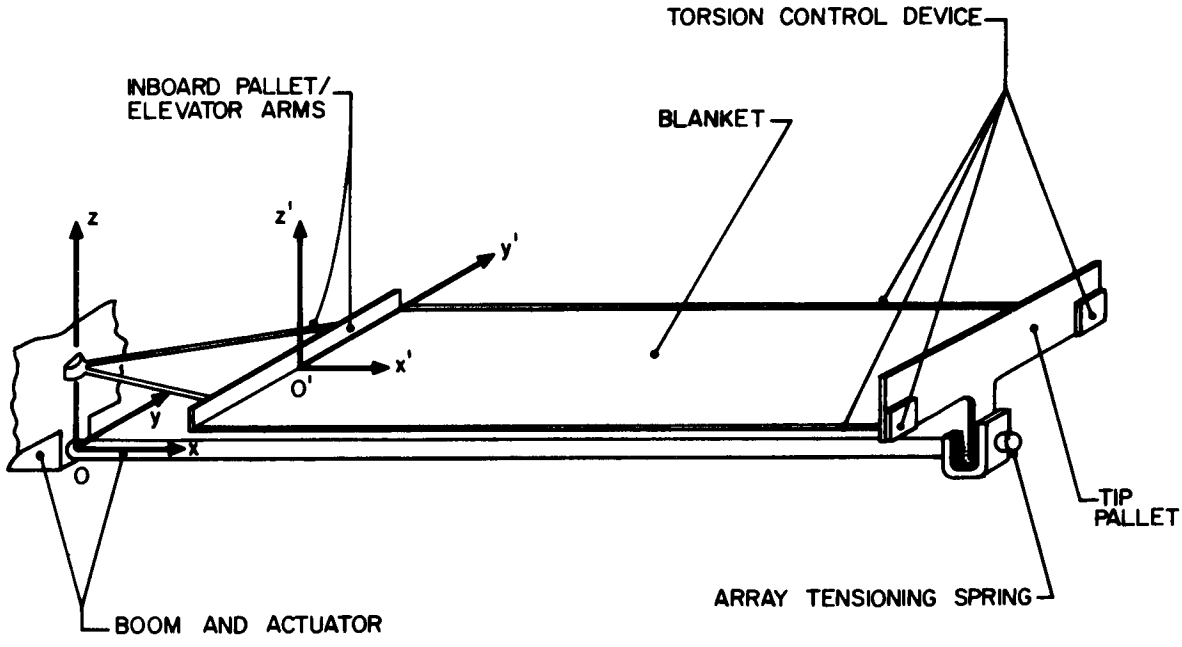


*Figure 1. Solar Array Assembly*

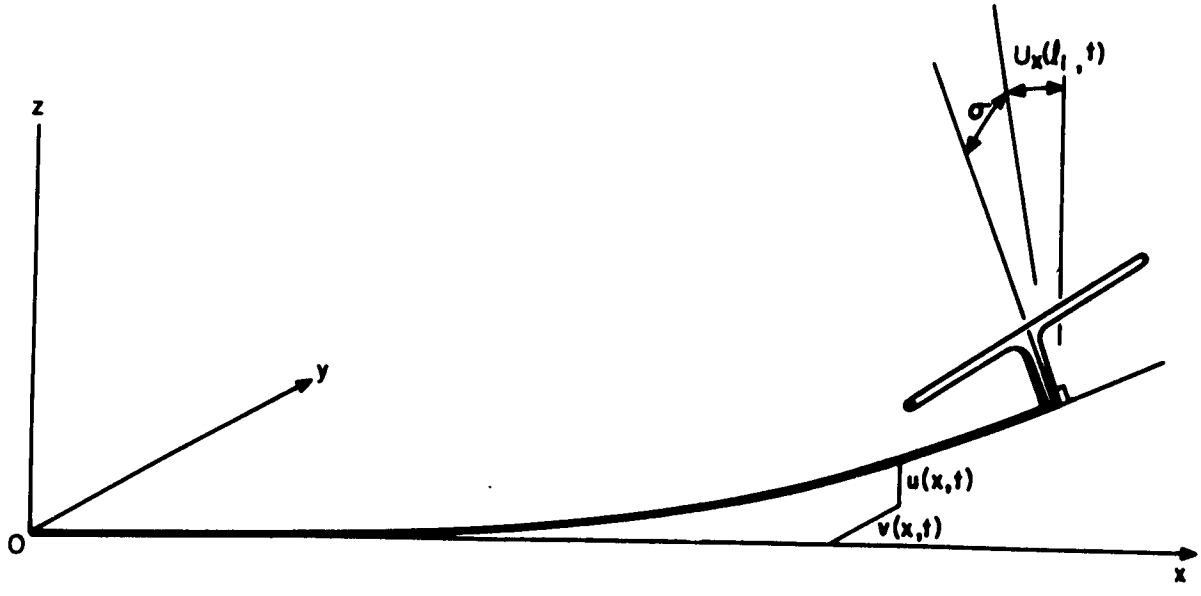


*Figure 2. Coordinates Specifying Boom and Tip Pallet Deformation*

*Table 1. Solar Array Parameters*

| Parameter | Array No. 1* | Array No. 2** |
|---|---|---|
| $\ell_1$ (ft) | 20.75 | 23.79 |
| $\ell_2$ (ft) | 18.0 | 21.33 |
| b (ft) | 4.0 | 4.30 |
| $\rho_1$ (slug/ft) | 0.00208 | 0.006052 |
| $\rho_2$ (slug/ft) | 0.00472 | 0.0204 |
| $m_1$ (slug) | 0.249 | 0.267 |
| $m_2$ (slug) | 0.14 | 0.0914 |
| $I_{px}$ (slug-ft$^2$) | 0.2314 | 0.41 |
| $I_{py}$ (slug-ft$^2$) | 0.0149 | 0.0195 |
| $I_{pz}$ (slug-ft$^2$) | 0.231 | 0.41 |
| e (ft) | 0.2 | 0.2 |
| a (ft) | 0.479 | 0.563 |
| $k_{r1}$ (lb-ft/rad) | ----- | 1100 |
| $k_{r2}$ (lb-ft/rad) | ----- | 2200 |
| $k_2$ (lb-ft) | 864. | 200 - 1500 (1200***) |
| $k_3$ (lb-ft) | $\infty$ | 100 - 1000 (100***) |
| $f_a$ (lb) | 1.0 | 2. - 5. (2.***) |
| $EI_1$ (lb-ft$^2$) | | 2320. |
| $EI_2$ (lb-ft$^2$) | | 2640. |
| JG (lb-ft$^2$) | 0. | 0 -20 (19.8***) |
| g (ft/sec$^2$) | 32.2 | 32.2 |
| $f_o$ (lb) | ------- | 0.20 - 0.75 (0.20***) |
| b' (ft) | 4.0 | 3. - 4.3 (3.5***) |

* *a dummy array made at CRC, with low quality hardware and manufacturing techniques.*

** *an array consisting of the CTS Preliminary Model Blanket (manufactured by AEG-TeleFunken) and the CTS Developmental Model Support Assembly (manufactured by SPAR Aerospace Co. Ltd.)*

*** *Value used to compute results shown in Table 2.*

## 2.2 BLANKET

The blanket of the CTS solar array, which consists of solar cell modules, instrumentation wiring, and bus bar wiring mounted on a kapton-fiberglass substrate, is modeled as a homogeneous membrane in which fibers are inextensible in the longitudinal direction.

Deformation in the out-of-plane (O'z') direction is assumed to be representable via,

$$w(x';y';t) = \zeta(x';t) + y'\alpha(x';t) \quad ; \tag{2}$$

that is, a translational deformation, $\zeta(x';t)$ of the blanket centerline, and a torsional deformation $\alpha(x';t)$, about the blanket centerline. The functions $\zeta$ and $\alpha$ are illustrated in Figure 3.

It is assumed that in-plane (Oy) deformation (warping) of the membrane is negligible compared to in-plane deformation incurred as a result of flexibility of the inboard pallet and elevator arms assembly. The blanket displacement in the in-plane direction is defined by specifying $\chi(t)$ and $\beta(t)$ (Figure 3). Deformation of the points in the blanket in the Ox direction, $\varepsilon_b(x';y';t)$, (due to foreshortening effects of the (inextensible) fibers, which accompany $\zeta$, $\alpha$, and $\beta$), is given approximately (see for example, Ref. 10) by,

$$\varepsilon_b(x';y';t) = - y'\beta - (h + x')\beta^2/2 - \frac{1}{2}\int_0^{y'} \{\zeta(x';t) + y\alpha(x';t)\}^2 dy \tag{3}$$

The membrane strain energy associated with deformations of the type described above is approximately invariant.

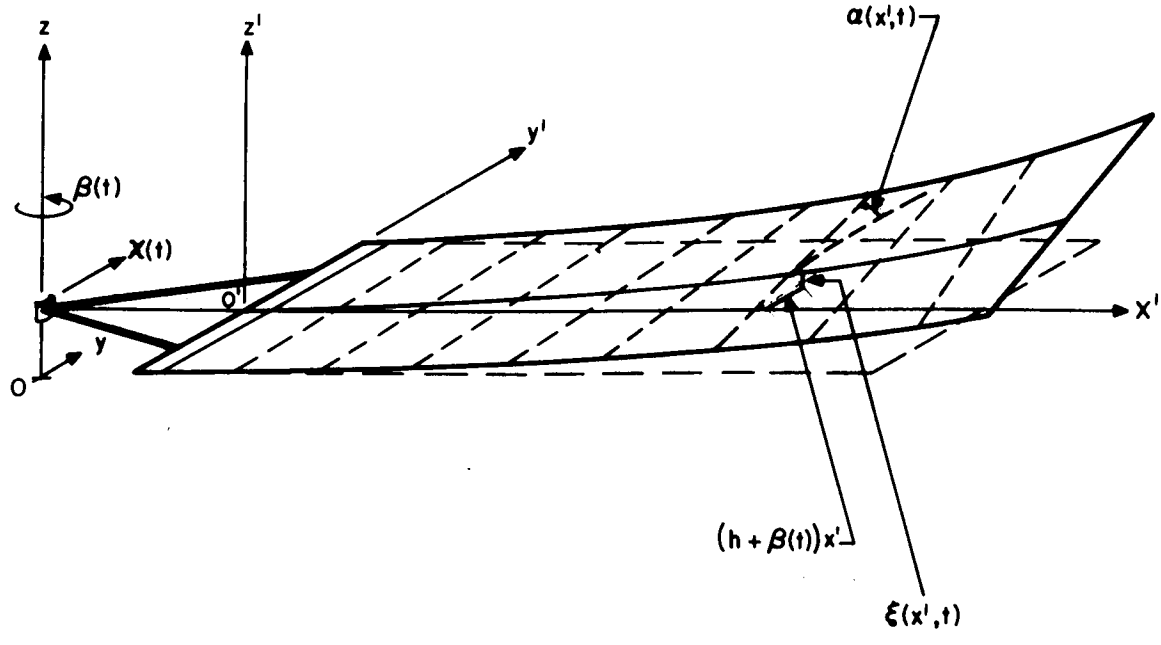


*Figure 3. Coordinates Specifying Blanket Deformation*

Blankets associated with the CTS program are expected to experience a state of non-uniform tension in ground test and on-orbit conditions, as a result of: (a) tolerances and shrinkage of various components of the blanket during manufacture; (b) manufacturing tolerances on curvature of inboard and tip pallets; (c) detail and assembly procedure of the blanket-to-tip pallet and blanket-to-base pallet connections; (d) slight flexibility of pallets; (e) variations in thickness and elastic modulus between cell regions, wiring areas, and kapton backing; (f) differential thermal expansions between various regions of the blanket, in ground, on-orbit sunlight, and on-orbit eclipse environments; (g) variation of tension distribution with twist (i.e., with $\alpha(x')$) in accordance with the non-linear phenomenon known as 'the shortening effect'[8]. The variation in longitudinal tension in the y' direction has a particularly significant influence on the torsional stiffness of the blanket and pallets combination. For example one may easily visualize two extreme cases: first, the torsional stiffness vanishes when the blanket longitudinal tension is concentrated along the centerline of the blanket, $y'=0$; and second, a maximum resistance to torsion occurs when the blanket longitudinal tension is concentrated at the two edges of the blanket, $y'=\pm b/2$. In principle, it is possible to model this mechanism; studies using the finite element method[9] and other techniques have established an understanding of the role that factors (d) - (g) play. However, for the present CTS design, it does not appear practical to model in detail for purposes of prediction, because factors (a) - (e), (and in particular, (a) - (c)), are not measurable or controlled to the degree required to justify an elaborate model. The net effect of factors (a) - (g) will be accounted for herein approximately, via the concept of "effective width b'", where $0 \leq b' \leq b$. The necessity of calculating the tension distribution is avoided as a result of this conceptual approximation in combination with the assumption that the longitudinal fibers of the blanket are inextensible. The torsional stiffness ranges over the two extremes cited above, in accordance with the available domain of b! The choice of b' is then a matter of engineering judgement, and may be decided upon on the basis of sensitivity studies, separate restricted analyses, and available test and manufacturing information.

## 2.3 INBOARD PALLET AND ELEVATOR ARMS

The inboard pallet and elevator arms form a truss-like structure having resistance to distortion in the in-plane (Oy) direction. The strain energy associated with deformation of this component has the form

$$\frac{1}{2} k_2 \beta^2 \tag{4}$$

The parameter, $k_2$, for the CTS array, is derived by direct measurement in a bench-test setup.

## 2.4 TIP PALLET

The tip pallet is assumed to be rigid. It is assumed to connect to the boom in a manner such that a right angle is maintained between the boom centerline, and the line on the pallet which joins the boom connection point

and the pallet center of mass (Figure 2). The connection between the tip pallet and blanket is assumed to have in-plane flexibility, as is consistent with a strain energy,

$$\frac{1}{2} k_3 \{v_x (\ell_1, t) - \beta(t)\}^2 \tag{5}$$

The contribution of Eqn. (5) is included for the purpose of accounting for the net effect of boom end local flexibility, tip pallet flexibility, and in-plane local warping of the blanket at the blanket-tip pallet connection. A quantitative value for $k_3$ is not readily deduced by direct measurement; the choice is a matter of engineering judgement, and in CTS application is decided upon to a large extent by matching calculations and array vibration results of Ref. 3. The pallet center of mass is assumed to lie on a line joining the centerline of the blanket and the boom. The principal axes of the pallet are assumed parallel to Oxyz when the solar array is underformed.

The pallet is assumed to connect to the blanket over the effective width, b', as discussed in section 2.2.

## 2.5 ARRAY TENSIONING SPRING

The array tensioning spring is assumed to be a constant force spring device, connecting and acting between the pallet and the boom (Figure 1). The spring is activated (removed from its stops) by the deployment action of the boom in the latter stage of the solar array deployment process. The work associated with this mechanism is

$$f_a \varepsilon \tag{6}$$

The constant, $f_a$, for the CTS array is derived by direct measurements.

## 2.6 TORSION CONTROL DEVICE

The torsion control device, which consists of negator springs and two lines connecting the tip-pallet edges with the inboard pallet, is modeled as a constant tension device. It will also be assumed that the lines coincide with the contours of the blanket edges under all circumstances. The net work done by the device when deformation occurs is,

$$2 f_o \varepsilon_T \tag{7}$$

The constant, $f_o$, is derived in the CTS program by direct measurement.

## 3. CONFIGURATION AND METHOD OF GROUND TEST

The ground test configuration[2,3] is depicted in Figure 4. The array is suspended inside CRC's 10' x 30' vacuum chamber with the 0x axis parallel with the earth's gravitational field vector. The array is excited with a hydraulic actuator, which can induce motion in three ways:

(a) out-of-plane excitation - oscillating translation of the boom and elevation arm base points along the 0z direction, i.e., a forced boundary condition imposed on u(x,t) and w(x¦y¦t),

$$u(0,t) = w(0,y¦t) = U(t); \quad u_x(0,t) = 0; \tag{8}$$

(b) in-plane excitation - oscillatory translation of the base of the boom and elevation arms along the 0y direction; i.e. a forced boundary condition is imposed on v(x,t),

$$v(0,t) = V(t); \quad v_x(0,t) = 0, \tag{9a}$$

and a corresponding motion $\chi(t)$ (Figure 3), of

$$\chi(t) = V(t) \tag{9b}$$

(c) torsional excitation - oscillatory rotation of the boom base about the 0x line; i.e. a forced boundary condition is imposed on the boom,

$$\sigma = \sigma_0(t), \tag{10a}$$

and a corresponding motion, $\chi(t)$ (Figure 3), of

$$\chi(t) = - e\, \sigma_o(t) \quad . \tag{10b}$$

## 4. POTENTIAL ENERGY, KINETIC ENERGY, AND CONSTRAINT EQUATIONS

### 4.1 CONSTRAINTS AMONG VARIABLES

The variables cited to describe the array component motions in the preceeding sections, namely $\{u(x,t), v(x,t), \sigma(t), \zeta(x¦t), \alpha(x¦t), \beta(t), \varepsilon_a, \varepsilon, \chi(t), U(t), v(t), \sigma_o(t)\}$, are not independent. The following relationships, approximated to linear order, exist among them.

$$\ell_1\beta(t) + e\{\alpha(\ell_2,t) - \alpha(0,t)\} = v(\ell_1,t) - V(t) \tag{11}$$

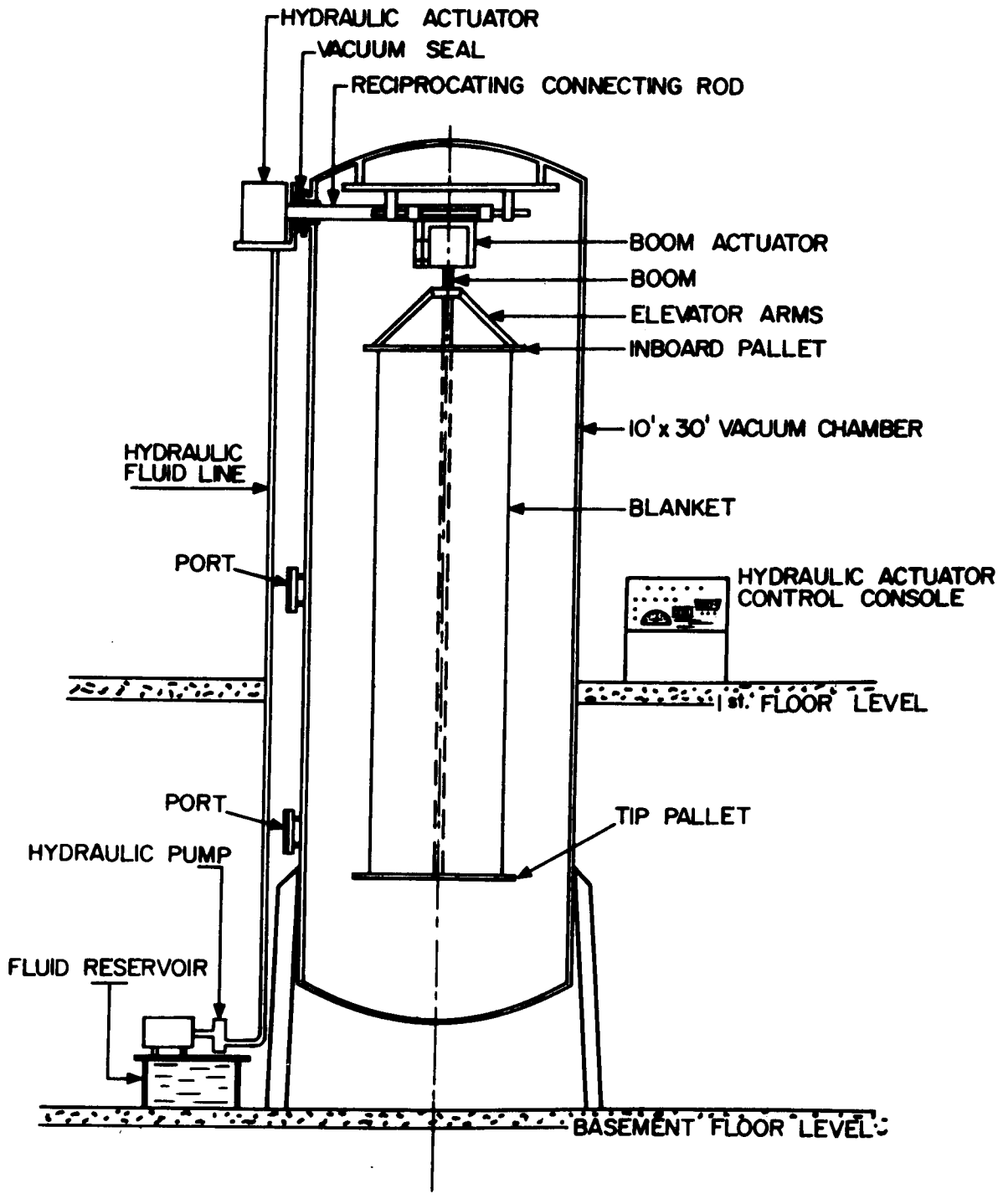


*Figure 4. Ground Test Configuration*

$$u(\ell_1,t) = \zeta(\ell_2,t) \tag{12}$$

$$\alpha(\ell_2,t) = \sigma(t) \tag{13}$$

$$\alpha(0,t) = \sigma_o(t) \tag{14}$$

$$\chi(t) = V(t) - e\,\sigma_o(t) \tag{15}$$

Deformations $\zeta(x;t)$ and $\alpha(x;t)$ of the blanket result in a decrease in the distance between the (rigid) tip pallet and the (rigid) inboard pallet, approximately by the amount

$$\frac{1}{2}\left[\frac{1}{2}\int_0^{\ell_2}\{\zeta_x + (b'/2)\alpha_x\}^2 dx + \frac{1}{2}\int_0^{\ell_2}\{\zeta_x - (b'/2)\alpha_x\}^2 dx\right] .$$

The above expression, together with similar ones which describe foreshortening associated with the boom, may be utilized to obtain,

$$\varepsilon = \ell_1\beta^2/2 + \frac{1}{2}\int_0^{\ell_2}\{\zeta_x^2 + (b'^2/4)\,\alpha_x^2\}dx - \frac{1}{2}\int_0^{\ell_1}(u_x^2 + v_x^2)dx$$

$$- e\,u_x\,(\ell_1,t) + e(\sigma - \sigma_o)\beta \tag{16}$$

Eq. (16) is valid to quadratic order of approximation in the variables which define the deformation.

The amount that the torsion control lines are extended off of their internal reels when blanket deformation occurs is $\varepsilon_T$, and is found by direct consideration of the kinematics of foreshortening, to be (provided that blanket is under tension),

$$\varepsilon_T = \frac{1}{2}\int_0^{\ell_2}\{(b^2 - b'^2)\,\alpha_x^2/4\,dx\} \tag{17}$$

The relation between blanket tension, $f_o$, and $f_a$, is (provided that the boom is deployed sufficient to ensure that the array tensioning spring is operative)

$$f_a = T_o + 2f_o - m_1 g \tag{18}$$

Since $f_a$ and $f_o$ are constant and determined during design and manufacture by the choice of negator springs, it follows that $T_o$ is constant and determined by choice of hardware components.

## 4.2 POTENTIAL ENERGY

The work (negative potential energy) done by gravity on the boom, incurred as elements of the boom foreshorten upwards with deformation (see for example, Ref. 8), is given by

$$-\frac{1}{2}\rho_1 g \int_0^{\ell_1}\int_0^{x}(u_x^2 + v_x^2)\,dx'\,dx \tag{19}$$

Similarly when the blanket deforms, points in it rise vertically due to foreshortening in accordance with Eq. (3). The corresponding work (negative potential) done by gravitational forces is,

$$-\frac{1}{2}\rho_2 g \int_0^{\ell_2}(h + x')\beta^2\,dx' - \frac{1}{2}\rho_2 g \int_0^{\ell_2}\int_0^{x}\{\zeta_x^2 + (b^2/12)\alpha_x^2\}\,dx'\,dx \tag{20}$$

The center of mass of the tip pallet moves vertically with deformation, incurring work (negative potential),

$$-m_1 g\left\{\frac{1}{2}\int_0^{\ell_1}(u_x^2 + v_x^2)dx + a\,u_x(\ell_1,t) - a\,(\sigma - \sigma_o)\beta + \varepsilon\right\} \tag{21}$$

Similarly the inboard pallet experiences the following work with deformation;

$$-m_2 g\,h\,\beta^2/2\ . \tag{22}$$

The potential energy of the array is comprised of the summation of contributions of Eqs. (1), (4 - 7), and (19 - 22). Combining these equations, together with Eqs. (11 - 14), (16), and (17), results in,

$$V = \frac{1}{2}\int_0^{\ell_1}(EI_1 u_{xx}^2 + EI_2 v_{xx}^2)dx + \frac{1}{2}JG\,\{\alpha(\ell_2,t) - \alpha(0,t)\}^2/\ell_1$$

$$+\frac{1}{2}\{k_2 + m_2 gh + (f_a + m_1 g)\ell_1 + \frac{1}{2}\rho_2\ell_2 g\,(\ell_2 + 2h)\}\beta^2$$

$$+\frac{1}{2}k_3\{v_x(\ell_1,t) - \beta\}^2 + \frac{1}{2}(f_a + m_1 g)\int_0^{\ell_2}\{\zeta_x^2 + (b'^2/4)\alpha_x^2\}\,dx$$

$$+ \frac{1}{2}\rho_1 g \int_0^{\ell_1}\int_0^{x} (u_x^2 + v_x^2)\, dx'\, dx + \frac{1}{2}\rho_2 g \int_0^{\ell_2}\int_0^{x} \{\zeta_x^2 + (b^2/12)\alpha_x^2\}\, dx'\, dx$$

$$- f_a \int_0^{\ell_1} (u_x^2 + v_x^2)\, dx + \{m_1 g\,(e - a) + f_a e\}\,\{\alpha(\ell_2,t) - \alpha(0,t)\}\beta$$

$$- \{m_1 g\,(e - a) + f_a e\}\, u_x(\ell_1,t) + f_o \int_0^{\ell_2} \{(b^2 - b'^2)\alpha_x^2/4\}\, dx \qquad (23)$$

## 4.3 KINETIC ENERGY

The kinetic energy of the boom, blanket, tip pallet, and inboard pallet, may be derived in the form,

$$T = \frac{1}{2}\rho_1 \int_0^{\ell_1} (\dot{u}^2 + \dot{v}^2)\, dx + \frac{1}{2}\rho_2 \int_0^{\ell_2} \{\dot{\zeta}^2 + (b^2/12)\dot{\alpha}^2\}\, dx$$

$$+ \frac{1}{2} I_z \dot{\beta}^2 + \frac{1}{2} m_1 \dot{u}^2\,(\ell_1,t) + \frac{1}{2}\{I_{py} + m_1(e - a)^2\}\,\dot{u}_x^2\,(\ell_1,t)$$

$$+ \frac{1}{2}\{I_{px} + m_1(e - a)^2\}\dot{\alpha}^2(\ell_2,t) + m_1\ell_1(e - a)\dot{\beta}\;\dot{\alpha}(\ell_2,t)$$

$$+ [m_1\ell_1 + \rho_2\ell_2\,\{h + (\ell_2/2)\} + m_2 h]\,\{\dot{V}(t) - e\,\dot{\sigma}_o(t)\}\,\dot{\beta}$$

$$+ m_1(e - a)\,\{\dot{V}(t) - e\dot{\sigma}_o(t)\}\,\dot{\alpha}(\ell_2,t)$$

$$+ \frac{1}{2}(m_1 + \rho_2\ell_2 + m_2)\,\{\dot{V}(t) - e\dot{\sigma}_o(t)\}^2 \qquad (24)$$

where

$$I_z = m_1\ell_1^2 + \rho_2\ell_2\,\{h + (\ell_2/2)\}^2 + m_2 h^2 + I_{pz} + \rho_2\ell_2\,\{(\ell_2/12) + (b^2/12)\}.$$

# 5. DISCRETIZATION

## 5.1 SERIES EXPANSIONS AND DISCRETE VARIABLES

The potentials and constraints of the previous section, expressed in terms of continuum coordinates, may be discretized via the assumption that each variable is representable by a series, the individual terms of which are products composed of a time-varying function and an assumed shape function. Specifically, the assumed composition of functions is,

$$u(x,t) = U(t) + \Phi^T \overline{u} \tag{25a}$$

$$v(x,t) = V(t) + \nu^T \overline{v} \tag{25b}$$

$$\zeta(x',t) = U(t) + \Psi^T \overline{\zeta} \tag{25c}$$

$$\alpha(x',t) = \sigma_o(t) + \Lambda^T \overline{\alpha} \quad , \tag{25d}$$

The above expressions are chosen in such a manner as to satisfy identically the boundary conditions cited in Eqs. (8 - 10). The functions $\overline{u}$, $\overline{v}$, $\overline{\zeta}$, and $\overline{\alpha}$ are column matrices with scalar time-varying elements, of order $N_u$, $N_v$, $N_\zeta$, and $N_\alpha$;

$$\overline{u}^T = [\overline{u}_1(t), \overline{u}_2(t), \ldots, \overline{u}_{N_u}(t)] \tag{26}$$

and so forth. The functions $\Phi$, $\nu$, $\Psi$, and $\Lambda$ are column matrices with spatially dependent (known) elements of order $N_u$, $N_v$, $N_\zeta$, and $N_\alpha$;

$$\Phi^T = [\Phi_1(\xi), \Phi_2(\xi), \ldots \Phi_{N_u}(\xi)] \ . \tag{27}$$

and so forth. The variable $\xi$, defined on the interval [0,1], substitutes for $x/\ell_1$, or $x'/\ell_2$ as appropriate. Derivatives of the elements are have the forms,

$$d\Phi_1(\xi)/dx = (d\Phi_1/d\xi)\ (d\xi/dx) = \Phi_\xi/\ell_1 \tag{28a}$$

$$d^2\Phi_1(\xi)/dx = \Phi_{\xi\xi}/\ell_1^2 \ ; \tag{28b}$$

and so forth. The function sets are assumed to be complete sets which satisfy,

$$\Phi(0) = \Phi_\xi(0) = \nu(0) = \nu_\xi(0) = 0 \tag{29a}$$

$$\Psi(0) = \Lambda(0) = 0 \quad , \tag{29b}$$

in accordance with Eqs. (8) and (9).

The time dependent variables may be further cast into matrix form,

$$Z = [\bar{u}^T | \bar{v}^T | \bar{\zeta}^T | \bar{\alpha}^T | \beta]^T \ . \tag{30}$$

## 5.2 POTENTIAL ENERGY

Substitution of Eq. (25) into Eq. (23), and further reduction to express the final result in terms of variable Z, leads to V in the form,

$$V = \frac{1}{2} Z^T KZ - G^T Z \ . \tag{31}$$

In Eq. (31), K is a matrix of order $(N_u + N_v + N_\zeta + N_\alpha + 1)^2$, composed of subelements with format,

$$K = \begin{bmatrix} K_{uu} & K_{uv} & K_{u\zeta} & K_{u\alpha} & K_{u\beta} \\ K_{vu} & K_{vv} & K_{v\zeta} & K_{v\alpha} & K_{v\beta} \\ K_{\zeta u} & K_{\zeta v} & K_{\zeta\zeta} & K_{\zeta\alpha} & K_{\zeta\beta} \\ K_{\alpha u} & K_{\alpha v} & K_{\alpha\zeta} & K_{\alpha\alpha} & K_{\alpha\beta} \\ K_{\beta u} & K_{\beta v} & K_{\beta\zeta} & K_{\beta\alpha} & K_{\beta\beta} \end{bmatrix} \tag{32}$$

The non-zero subelements of K are,

$$K_{uu} = (EI_1/\ell_1^3)B^\Phi + \rho_1 g\, H^\Phi - (f_a/\ell_1)\, J^\Phi$$

$$K_{vv} = (EI_2/\ell_1^3)B^\Phi + \rho_1 g\, H^\nu - (f_a/\ell_1)\, J^\nu + (k_3/\ell_1^2)\nu_\xi(1)\, \nu_\xi^T(1)$$

$$K_{\zeta\zeta} = \{(f_a + m_1 g)\, J^\Psi/\ell_2\} + \rho_2 g\, H^\Psi$$

$$K_{\alpha\alpha} = JG\Lambda(1)\Lambda^T(1)/\ell_1 + \{(f_a + m_1 g)b'^2\, J^\alpha/4\ell_2\} + \{\rho_2 g b^2\, H^\alpha/12\} + f_o(b^2 - b'^2)J^\alpha/2\ell_2$$

$$K_{\beta\beta} = k_2 + k_3 + m_2 gh + (f_a + m_1 g)\,(\ell_2 + h) + \rho_2 \ell_2 g\, \{(\ell_2 + 2h)/2\}$$

$$K_{v\beta} = K_{\beta v}^T = -\, k_3\, \nu_\xi(1)/\ell_1$$

$$K_{\alpha\beta} = K_{\beta\alpha}^T = \{m_1 g\ (e - a) + f_a\ e\}\ \Lambda(1) \quad ,$$

where the functionals B, H, and J are defined as,

$$B^p = \int_0^1 p_{\xi\xi}\ p_{\xi\xi}^T\ d\xi \tag{33}$$

$$H^p = \int_0^1 \int_0^\xi p_\xi\ p_\xi^T\ d\xi'\ d\xi \tag{34}$$

$$J^p = \int_0^1 p_\xi\ p_\xi^T\ d\xi \quad . \tag{35}$$

The matrix, G, of order $(N_u + N_v + N_\zeta + N_\alpha + 1) \times 1$, has format

$$G = [G_u^T,\ G_v^T,\ G_\zeta^T,\ G_\alpha^T,\ G_\beta^T]^T \quad , \tag{36}$$

and non-zero elements

$$G_u = \{m_1 g\ (e - a) + f_a e\}\ \Phi_\xi(1)/\ell_1 \quad . \tag{37}$$

## 5.3 KINETIC ENERGY

Substitution of Eqs. (25) into Eq. (24), and condensation of the result yields,

$$T = \frac{1}{2}\ \dot{Z}^T\ M\ \dot{Z} - F^T\dot{Z} + T_1(t) \quad , \tag{38}$$

where $T_1(t)$ is a time-varying function, M is a matrix of order $(N_u + N_v + N_\zeta + N_\alpha + 1)^2$ whose subelements have a format similar to K of Eqn. (32). The non-zero elements are

$$M_{uu} = \rho_1 \ell_1 \Xi^\Phi + m_1\ \Phi(1)\ \Phi^T(1) + [\{I_{py} + m_1\ (e - a)^2\}\Phi_\xi(1)\ \Phi_\xi^T(1)/\ell_1^2]$$

$$M_{vv} = \rho_1 \ell_1 \Xi^\nu$$

$$M_{\zeta\zeta} = \rho_2 \ell_2 \Xi^{\Psi}$$

$$M_{\alpha\alpha} = (\rho_2 \ell_2 b^2/12)\Xi^{\Lambda} + \{I_{px} + m_1(e - a)^2\}\ \Lambda(1)\ \Lambda^T(1)$$

$$M_{\beta\beta} = I_z$$

$$M_{\alpha\beta} = M_{\beta\alpha}^T = m_1 \ell_1\ (e - a)\ \Lambda(1) \quad . \tag{39}$$

F is of format of Eq. (36), with elements

$$F_u = -\{\rho_1 \ell_1\ Q^{\Phi} + m_1\ \Phi(1)\}\ \dot{U}(t)$$

$$F_v = -\rho_1 \ell_1\ Q^{\nu}\ \dot{V}(t)$$

$$F_\zeta = -\rho_2 \ell_2\ Q^{\Psi}\ \dot{U}(t)$$

$$F_\alpha = -[(\rho_2 \ell_2 b^2/12)\ Q^{\Lambda} + \{I_{pz} + m_1(e - a)^2\}\ \Lambda(1)]\ \dot{\sigma}_o(t)$$

$$- m_1(e - a)\ (\dot{V} - e\ \dot{\sigma}_o)\ \Lambda(1)$$

$$F_\beta = m_1 \ell_1\ (e - a)\ \ \dot{\sigma}_o(t) + [m_1 \ell_1 + \rho_2 \ell_2\ \{\ell_1 + \ell_2/2\} + m_2 h]$$

$$\{\dot{V}(t) - e\ \dot{\sigma}_o(t)\} \tag{40}$$

In Eqs. (39) and (40), the functionals $\Xi$ and Q are defined by,

$$\Xi^P = \int_0^1 p(\xi)\ p^T(\xi)\ d\xi \tag{41}$$

$$Q^P = \int_0^1 p(\xi)\ d\xi \tag{42}$$

## 5.4 CONSTRAINT RELATIONS

The constraint relations expressed in Eqs. (13 - 15) of Section 4.1 are incorporated into the V and T of Eqns. (31) and (38). The remaining two relations, Eqns. (11) and (12), may be conveniently dealt with after discretization (via Eqns. (25)) when expressed as a coordinate transformation,

$$Z = \Pi z \quad , \tag{43}$$

where z is a column matrix of order $\{N_u + N_v + N_\zeta + N_\alpha - 1\}$ (i.e., of order N, the order of discretization of the total structure),

$$z = [\bar{u}^T, \bar{v}^T, \bar{\bar{\zeta}}^T, \bar{\alpha}^T]^T \quad , \tag{44}$$

and

$$\bar{\bar{\zeta}} = [\bar{\zeta}_1(t), \bar{\zeta}_2(t), \ldots . \bar{\zeta}_{N_{\zeta-1}}(t)]^T \quad . \tag{45}$$

$\Pi$, a matrix of order $\{(N+2) \times N\}$, is

$$\Pi = \begin{bmatrix} E^{\Phi} & 0 & 0 & 0 \\ 0 & E^{\nu} & 0 & 0 \\ 0 & 0 & E^{\psi-1} & 0 \\ \Pi_{41} & 0 & \Pi_{43} & 0 \\ 0 & 0 & 0 & E^{\Lambda} \\ 0 & \Pi_{62} & 0 & \Pi_{64} \end{bmatrix} \quad , \tag{46}$$

where $E^{\Phi}$, $E^{\nu}$, $E^{\psi-1}$, and $E^{\Lambda}$, are identity matrices of order $N_u$, $N_v$, $N_{\zeta-1}$, and $N_\alpha$, and the remaining elements are,

$$\Pi_{41} = \Phi^T(1)/\Psi_{N_\zeta}(1)$$

$$\Pi_{43} = -\bar{\bar{\Psi}}^T(1)/\Psi_{N_\zeta}(1)$$

$$\Pi_{62} = \nu^T(1)/\ell_1$$

$$\Pi_{64} = -e\Lambda^T(1)/\ell_1$$

In the above, $\Psi_{N_\zeta}(\xi)$ is the last scalar element in $\Psi$, and,

$$\bar{\bar{\Psi}}_N^T(1) = [\Psi_1(1), \Psi_2(1), \ldots\ldots \Psi_{N_{\zeta-1}}(1)] \quad . \tag{47}$$

## 6. EQUATIONS OF STATIC EQUILIBRIUM AND MOTION

The formulation at this point is embodied in V and T of Eqs. (31) and (38), and the constraint relation, Eq. (43). Substitution of Eq. (43) into Eqs. (31) and (38) results in elimination of the constraint equation, and correspondingly, T and V in the form,

$$V = \frac{1}{2} z^T \{\Pi^T K \Pi\} z - G^T \Pi z \tag{48}$$

$$T = \frac{1}{2} \dot{z}^T \{\Pi^T M \Pi\} \dot{z} - F^T \Pi \dot{z} + T_o(t) \tag{49}$$

We further consider z as composed of

$$z(t) = z_o + q(t) \quad , \tag{50}$$

the sum of a static shape, $z_o$, and a time-varying component, q(t). Substitution of Eq. (50) into Eqs. (48) and (49), and of the result into Hamilton's Principle,

$$\delta \int_{t_1}^{t_2} (T - V) dt = 0 \quad , \tag{51}$$

yields, to a linear order approximation,

$$z_o = (\Pi^T K \Pi)^{-1} \Pi^T G \tag{52}$$

$$\{\Pi^T M \Pi\} \ddot{q} + \{\Pi^T K \Pi\} q = \Pi^T \dot{F} \tag{53}$$

Thus the static shape may be calculated algebraically via Eqn. (52) and successive back-substitution through Eqs. (43), (30), and (25) (with U(t), V(t), $\sigma_o(t)$ taken equal to zero).

Vibrational frequencies and mode shapes may be obtained after solving the characteristic equation derivable from Eq. (53), namely,

$$\{(\Pi^T K \Pi) - \omega_n^2 (\Pi^T M \Pi)\} q_n = 0 \quad . \tag{54}$$

K and M are symmetric; it then follows that $\Pi^T M \Pi$ and $\Pi^T K \Pi$ are also symmetric ($\{\Pi^T M \Pi\}^T = \Pi^T \{\Pi^T M\}^T = \Pi^T M^T \Pi = \Pi^T M \Pi$). Consequently the eigenvalues of Eqn. (54) are real, and the eigenvectors, $q_n$, are mutually orthogonal.

Motion equations may be derived in terms of modal coordinates from Eq. (53) as follows. Assume a series decomposition for q:

$$q = \sum_{k=1}^{n} q_k \eta_k (t) \quad , \tag{55}$$

where $q_k$ are the eigenvectors corresponding to Eq. (54), and $\eta_k(t)$ are scalar coordinate functions. Substitution of Eq. (55) into Eq. (53), premultiplication by $q_m^T$, use of the above cited orthogonality property, and the usual addition of 'modal damping', results in for the $m^{th}$ mode:

$$\ddot{\eta}_m + 2\zeta_m \omega_m \dot{\eta}_m + \omega_m^2 \eta_m = (q_m^T \Pi^T F)/(q_m^T \Pi^T M \Pi q_m) \tag{56}$$

Eq. (56) together with the implied back substitution through Eqs. (55), (43), (30), and (25), thus constitute a mathematical model which describes the array structural dynamics. In Eq. (56), all quantities are calculable, with the exception of the damping factors $\zeta_m$. Estimates for $\zeta_m$'s for solar arrays, deduced from various test and analysis techniques, range from 0.001 to 0.02.

The modal functions, $q_k$, and associated $\omega_k$'s and $\zeta_k$'s (often referred to 'fixed base' or 'constrained' modes) also serve, for a particular array and spacecraft, as basic flexibility information and a first step in the analysis of spacecraft attitude dynamics.

## 7. APPLICATION IN CTS PROGRAM

### 7.1 CALCULATED FREQUENCIES AND MODE SHAPES

Static shape and lower order modes and frequencies have been obtained from Eqns. (52) and (54) by numerical means. The function sets chosen in Eqns. (25) were,

$$\Phi = [\xi^2, \xi^3, \xi^4]^T; \quad N_u = 3$$

$$\nu = [\xi^2, \xi^3, \xi^4]^T; \quad N_v = 3 \qquad (57)$$

$$\psi = [\xi, \xi^2, \xi^3,]^T; \quad N_\zeta = 3$$

$$\Lambda = [\xi, \xi^2, \xi^3,]^T; \quad N_\alpha = 3 \quad .$$

Sample solutions corresponding to parameters representative of the CTS Array No. 2 (Table 1) are illustrated in Figures 5 - 12 for situations where g = 32.2, and g = 0. The modes may be categorized in two classes; out-of-plane (boom and blanket vibrate in the Oz direction), and torsion/in-plane (the boom and blanket vibrate in the plane normal to the line Oz, accompanied by torsional deformation of the blanket). The two categories arise because in the mathematical model there is no coupling between the equations embodying these two separate types of motion.

## 7.2 COMPARISON OF NUMERICAL RESULTS WITH TEST DATA

Two physical models of array have been tested at CRC's David Florida Laboratory facilities, a "CRC Built" array[2] (Array No. 1) and a "CTS Developmental Model" array[3] (Array No. 2). Comparison of calculated and measured frequencies and mode shapes is given in Table 2 for sets of parameters listed in Table 1. The calculations shown do not exactly match the test results; however the residual disagreements are compensated for by the indeterminacy of some of the parameters shown in Table 1. The results demonstrate that the analytical model describes the major structural modes.

The results given in Table 2 are those obtained after a certain amount of 'adjusting' of the parameter values to optimize the agreement between theory and test. One might well ask, "how well can one expect to estimate the behaviour using the modeling only, in the absence of test data?". The uncertainty in numerical estimates provided via the modeling stems from two sources; first, shortcomings in the analytical representation of the hardware; and second, uncertainty in the numerical values of the parameters (e.g. moments of inertia, EI,JG, etc.). In this instance, it is our experience that the second factor is the dominant one by a healthy margin. In advance of testing, and with b'= b,$k_3 = \infty$: the three lowest 'out-of-plane' frequencies were correctly predicted to within 5 - 10%; the first and second in-plane/torsion frequencies were estimated to within 15% correctly; the third in-plane/torsion frequency was correctly estimated to within 35%; fourth out-of-plane and fifth torsion/in-plane frequencies were estimated within a factor of two. The structural mechanism associated with b' was essential for more accurate modeling of frequencies which have a large component of twisting motion (the second and third in-plane/torsion frequencies in this instance); the structural mechanism associated with $k_3$ was required for accurate description of modes in which the boom motion is the major component (fourth out-of-plane and fifth torsion/in-plane).

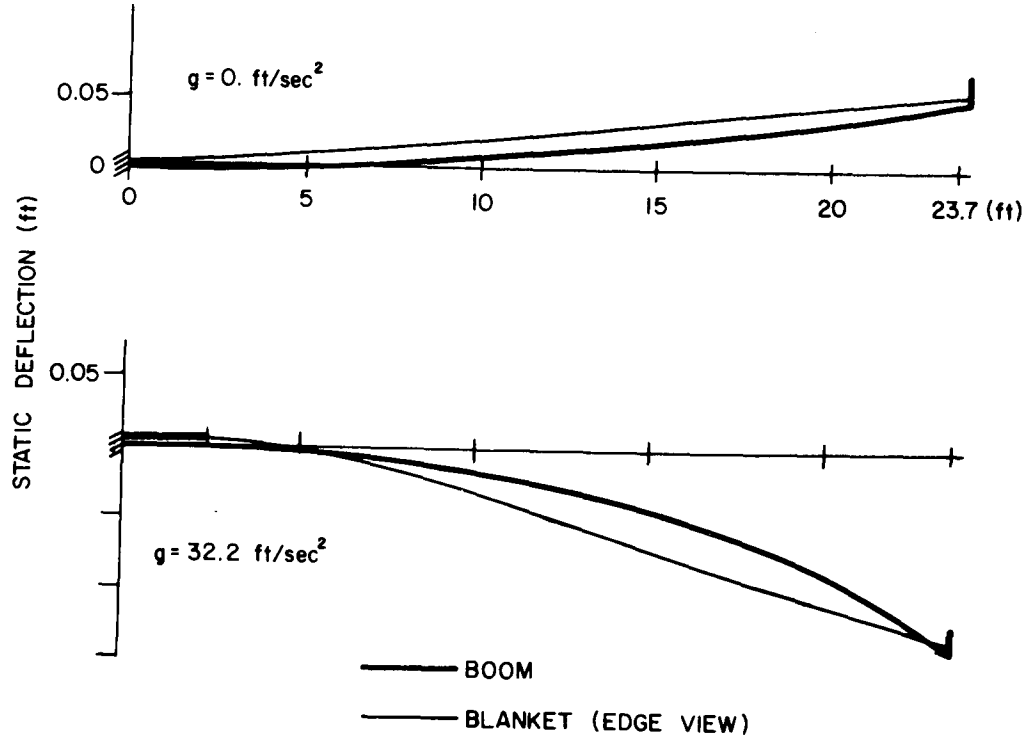


*Figure 5. Static Shape, g = 0, 32.2*

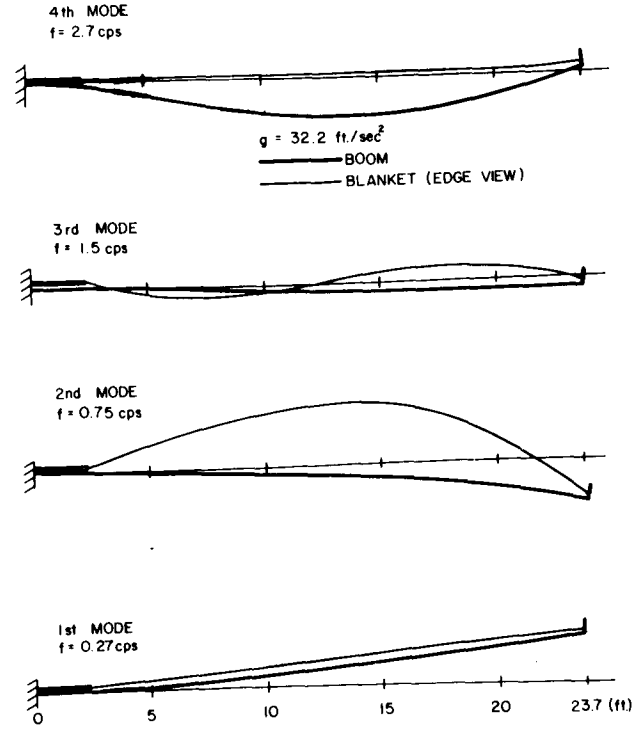


*Figure 6. Out-of-Plane Modes, g = 32.2ft/sec²*

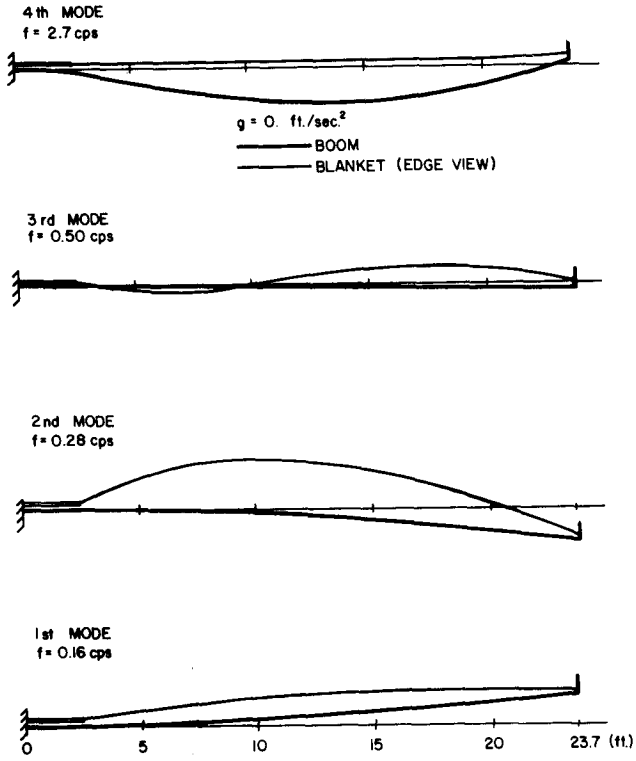


*Figure 7. Out-of-Plane Modes, g = 0 ft/sec²*

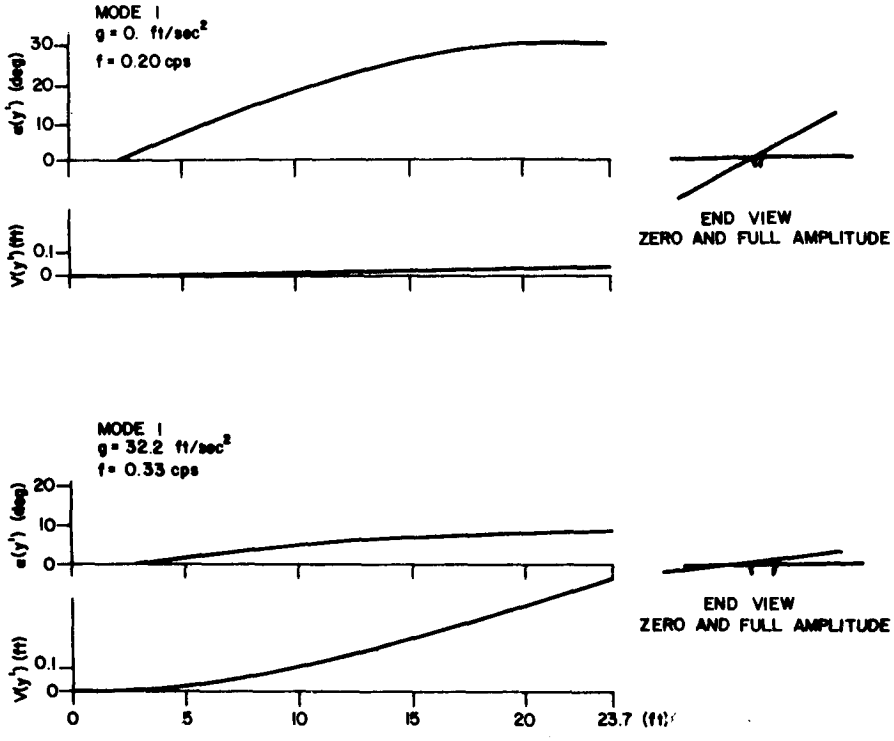


*Figure 8. In Plane – Torsion Mode 1, g = 0, 32.2*

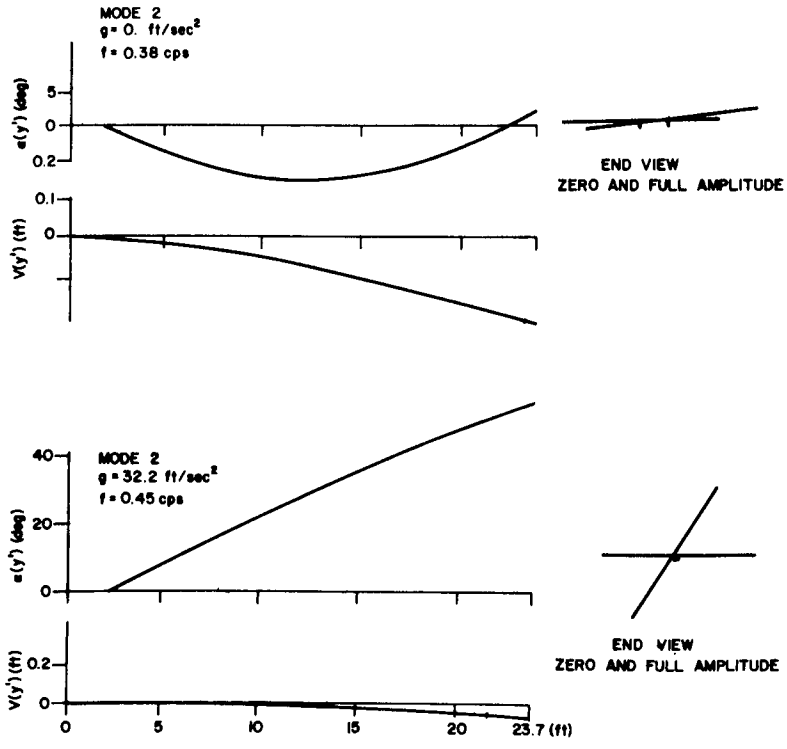


*Figure 9. In Plane — Torsion Mode 2, g = 0, 32.2*

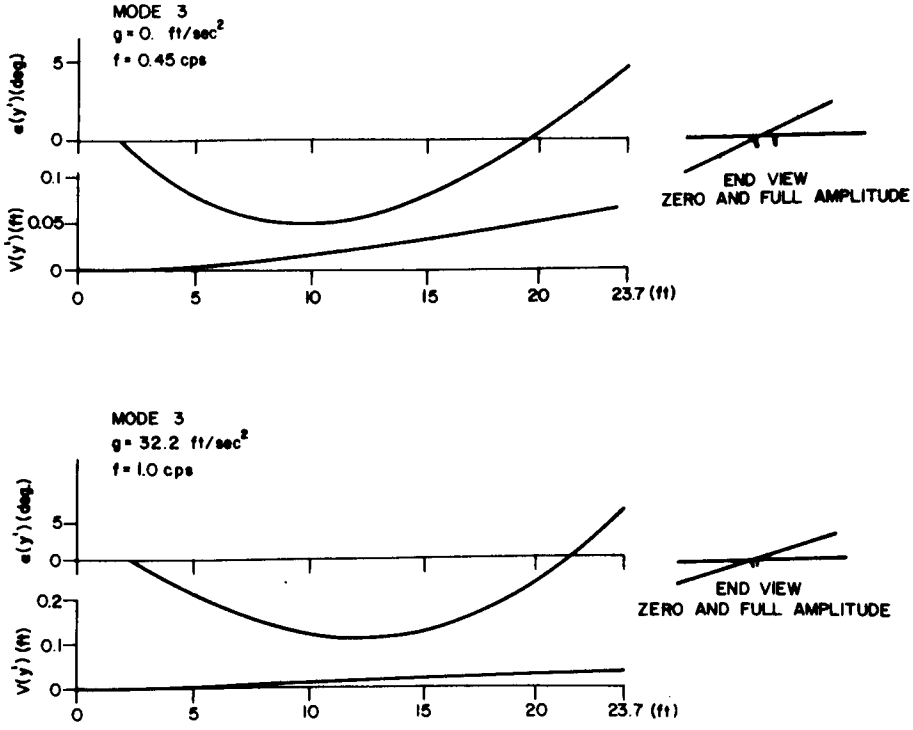


*Figure 10. In Plane — Torsion Mode 3, g = 0, 32.2*

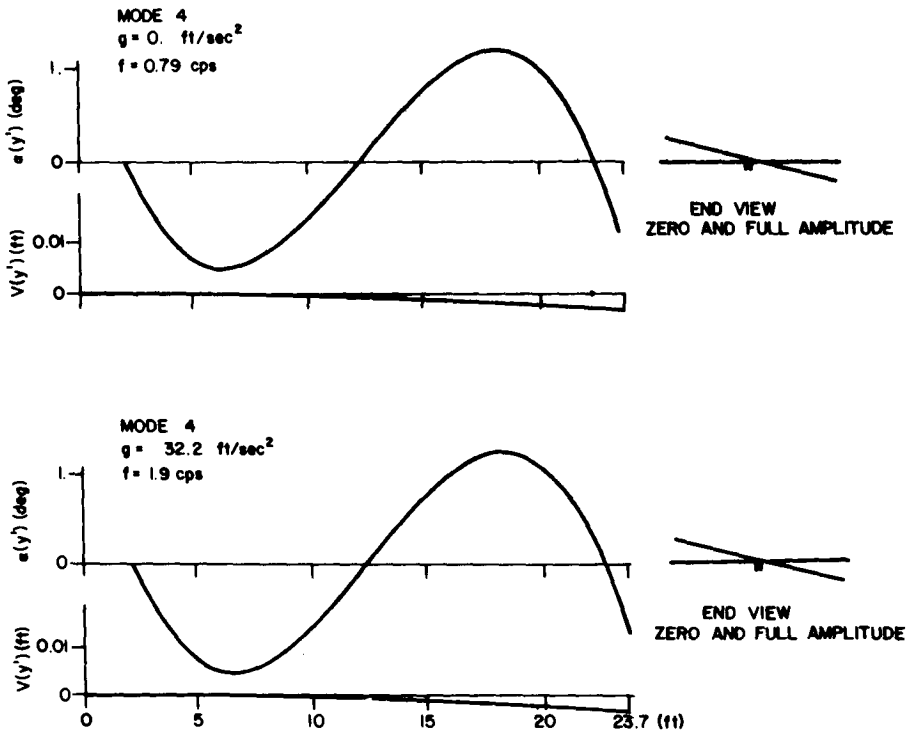


*Figure 11. In Plane – Torsion Mode 4, g = 0, 32.2*

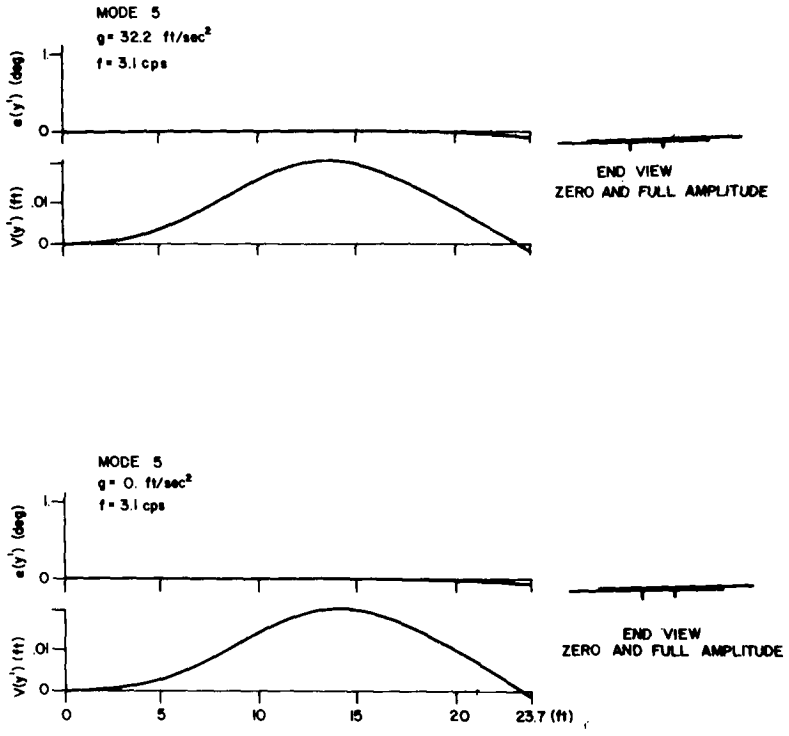


*Figure 12. In Plane – Torsion Mode 5, g = 0, 32.2*

*Table 2. Measured vs Calculated Results*

| Array | Type of Mode | Measured Frequency (Hz) | Measured damping coefficient (small ampl. / large ampl.) | Calculated Frequency (Hz) | Correspondence between calc. and measured mode shapes |
|---|---|---|---|---|---|
| Array No. 1 | 1st out-of-plane | 0.26 | 0.01 | 0.22 | good |
| | 2nd out-of-plane | 1.1 | not measured | 1.3 | good |
| | 1st torsion/in-plane | 0.33 | 0.01 | 0.35 | good |
| | 2nd torsion/in-plane | 0.48 | 0.005 | 0.42 | measured results had a higher ratio of torsion vs in-plane bending than calculated |
| | Membrane-type Blanket modes | 1.81, 1.88 | --------- | not calculated | |
| Array No. 2 | 1st out-of-plane | 0.27 | 0.004/0.01 | 0.27 | good |
| | 2nd out-of-plane | 0.74 | 0.002/0.02 | 0.75 | good |
| | 3rd out-of-plane | 1.3 | not measured | 1.5 | good |
| | 4th out-of-plane | 2.6 * | 0.003 | 2.7 | good |
| | 1st torsion/in-plane | 0.35 | 0.003/0.01 | 0.33 | good |
| | 2nd torsion/in-plane | 0.44 | not measured | 0.45 | good |
| | 3rd torsion/in-plane | 0.84 | 0.002 | 1.0 | good |
| | 4th torsion/in-plane | not detected | not measured | 1.9 | ---- |
| | 5th torsion/in-plane | 2.6 * | 0.003 | 3.1 | good |
| | Membrane-type Blanket modes (8) | 0.9;1.17;1.45; 1.65;1.92;2.; 2.4;2.65 | very low | not calculated | ---- |

* T.D. Harrison in Ref. 3 refers to a 'boom fundamental mode' a single mode which 'beats' in amplitude between in-plane and out-of-plane directions. After discussions with T.D. Harrison, the author formed the conclusion that the 'boom fundamental' actually was two separate modes which were very close in frequency.

The data given in Table 2 shows that the modeling does not account for the 'blanket modes' the latter being those in which the blanket vibrates as a membrane, more or less independent of the rest of the array. Separate analytical investigation of the unaccounted-for membrane-type modes shows that they are precluded in the modeling as a result of the form of assumed deflection function, w(x¦y¦t) of Eqn. (2). Separate analyses by the author show that these modes may be attributed to non-uniform (static) tension distribution in the plane of the blanket. The membrane-type blanket modes tend to be high in frequency and of low vibrational energy in comparison to the prime structural modes for the CTS design, and do not appear to be of prime consequence or concern from the viewpoint of attitude stabilization or structural design. The modeling of blanket modes appears tractable and easily handled via finite element techniques[9]. Accordingly, effort to update the version of the theory presented herein to incorporate the blanket modes does not appear justifiable.

The test results also show that fundamental array modes may be excited substantially by excitation at frequencies which are fractions of the modal frequencies. The modeling herein does not account for this feature. This phenomenon, namely superharmonic vibration, is a well established one for simple systems[11], and may probably be accounted for in the present context via non-linearities in structural stiffness or damping[12]. This feature is of potential significance in spacecraft design; for example, an attitude control system design with bandpass frequency lower than the natural frequencies of structural vibration could interact with structural vibrations via the excitation of superharmonic frequencies. The investigation of this feature is left for future study.

## 7.3 REMARKS ON PREDICTION OF ON-ORBIT ARRAY CHARACTERISTICS

The course adopted in the CTS program with respect to prediction of the large flexible array structural characteristics is one in which: (a) an analytical model of the array behaviour is developed and verified by test under one-g (earth) conditions; (b) the model is then used to predict zero-g (on-orbit) conditions.

One would expect the above approach to be a valid one when the modes, frequencies, and stress levels, at one-g and zero-g are of the same order of magnitude and qualitative feature. The calculations presented in Figures 5 - 12, illustrate that this condition is met in the present case. A factor associated with the boom which has not been reflected in the above calculations is 'boom root flexibility', a structural mechanism characteristic of STEM and BISTEM deployment actuator and boom devices. The factor accounts for flexibility associated with ovalling of the boom in the region of its root, and root flexibility in guidance rollers and related deployment hardware. The factor may be directly accounted for in the preceding development via appropriate definition of $EI_1$ and $EI_2$ as piecewise continuous functions of boom length. The CTS array under ground test is not particularly sensitive to this factor mainly because the stiffening influence of the one-g field tends to dominate and thus mask it. Numerical estimates show that, for the CTS array with boom root flexibility factors as indicated in Table 1, the influence is sufficiently small to be neglected. However, it would be prudent to account for this factor in extrapolations of this work to other applications.

## 7.4 COMMENTS ON ANALYSES OF REFS. 4 - 7

Modeling of the CTS array under zero-g conditions via the finite element method is documented in Ref. 4. The work of Ref. 4 was performed in 1970; since that time, the CTS array design has evolved and been modified to an extent where quantitive comparison of results with those herein is not meaningful. However qualitative agreement is evident. In particular one notes that the finite element method calculates the previously discussed membrane-like modes.

Modeling presented in Ref. 5 - 7 is subject to the limitation that the membrane-type blanket modes are precluded as a result of assumptions made in modeling the blanket. Also in these works, the assumption is made that the offset, e, may be ignored (taken as zero), which results in the three characteristic types of motion, namely twisting (torsion), out-of-plane and in-plane, being independent (uncoupled); this feature is not in agreement with the evidence of testing which indicates the twisting (torsion) and in-plane motions are coupled for the CTS array. The modeling presented in Ref. 5 further ignores the possibility of in-plane deformation of any form - this is not in accord with the observed CTS array characteristic behaviour. The structural mechanisms associated with the parameters $k_2$, $b'_1$ and $k_3$ are not included in the modeling of Refs. 5 and 7. The above variances result in the absence in the model, of "in-plane" modes and "torsion-in plane motion coupling". The modeling of Refs. 5 and 7 does not account for the observed superharmonic vibration characteristics of CTS Array No. 2.

# 8. CONCLUDING REMARKS

The modeling as presented herein describes the major features of structural dynamics of the CTS array under one-g (earth) test conditions. The modeling does not account for higher frequency membrane-type vibrations and superharmonic vibrations, two features which are observed in testing.

It is the author's view that the foregoing model may be extrapolated with confidence to predict the corresponding features of the structural dynamics of the CTS spacecraft in its on-orbit state.

The modeling may also be expected to be valid for a range of solar arrays of the CTS class - that is, arrays composed of a single boom and a membrane-like blanket.

# 9. ACKNOWLEDGMENTS

The author wishes to acknowledge contributions made to this work, by R. Cloutier and S. Zurawski in computer programming support, and by T.D. Harrison and A. Parthasarathy in the course of sorting out the correlation between analytical and test results.

## 10. REFERENCES


1. Franklin, C.A., and Davidson, E.H., *A High Power Communications Technology Satellite for the 12 and 14 GHz Bands*, AIAA Progress in Astronautics and Aeronautics, Vol. 32, MIT Press, 1973.

2. Private Communication, Harrison, T.D., *Solar Array Testing Program - Report on Phase I*, CRC Memorandum CRC 6666-15-1-6 (CTS) Program, 29 October 1973.

3. Harrison, T.D., *Communications Technology Satellite Deployed Solar Array Dynamics Tests*, CRC Report No. 1264, January 1975.

4. Remedios, E.E., and Yao, C.C., *Vibration Analysis of Deployable Solar Array Wing*, Ontario Research Foundation, Report No. ENG. R-70-112, Sheridan Park, Ontario, Canada.

5. Hughes, P.C., *Attitude Dynamics of a Three-Axis Stablized Satellite With a Large Flexible Solar Array*, Journal of the Astronautical Sciences, Vol. 20, No. 3, Nov. - Dec. 1972, pp 166 - 189.

6. Hughes, P.C., *Flexible Motions of the CTS Solar Array in the Plane of the Array*, Aerospace Engineering and Research Consultants Ltd., Report No. 70-41-2, Dec. 1970.

7. Cherchas, D.B., *Coupled Bending-Twisting Vibrations of a Single Boom Flexible Solar Array and Spacecraft*, CASI Transactions, Vol. 6, No. 1, March 1973, pp 56 - 60.

8. Cullimore, M.S.G., *The Shortening Effect - A Non-Linear Feature of Pure Torsion*, in Research, Engineering Structures, Colston Papers, Vol. II, Butterworth's Scientific Publications, London, 1949, pp 153 - 164.

9. Private Communication with A. Parthasarathy. Results to be submitted for publication as a CRC Report.

10. Vigneron, F.R., *Stability of a Freely Spinning Satellite of Crossed-Dipole Configuration*, Appendix B, CASI Transactions, Vol. 3, No. 1, March 1970, pp 8 - 18.

11. Abramson, H.N., *Nonlinear Vibrations* in Shock and Vibration Handbook, Vol. 1, McGraw-Hill (Edited by Harris and Crede), 1961, pp 4-1 to 4-36.

12. Bolotin, V.V., *The Dynamics Stability of Elastic Systems*, Holden-Day Inc., 1964.

# CRC DOCUMENT CONTROL DATA

1. ORIGINATOR: Space Technology Branch

2. DOCUMENT NO: CRC Report No. 1268

3. DOCUMENT DATE: April 1975

4. DOCUMENT TITLE: A Structural Dynamics Model for Flexible Solar Arrays of the Communications Technology Satellite

5. AUTHOR(s): F. Vigneron

6. KEYWORDS: (1) Solar Arrays
(2) Flexible
(3) Dynamics

7. SUBJECT CATEGORY (FIELD & GROUP: COSATI)

22 Space Technology

22 02 Spacecraft

8. ABSTRACT:

A mathematical model, which describes the structural mechanics of flexible solar arrays of the Communications Technology Satellite (CTS) in a ground test configuration, is developed using variational principles and continuum mechanics methods. Modes and frequencies for an array with CTS parameters are calculated for the one-g test state, and compared to corresponding ones for the zero-g on-orbit state. Calculated results are compared with ground test data; good agreement is noted for the major structural frequencies and modes. The model does not predict certain observed higher frequency membrane-like blanket modes attributable to non-uniform tension distribution in the solar array blanket. Also the test results show that modal frequencies may be excited by subharmonic excitation; this feature would necessitate a non-linear vibrational model, and is not accounted for in the mathematical model. Alternate mathematical models based on finite element and continuum mechanics methods, which were developed for the design phase of the CTS program, are discussed in the light of test data and modeling of this report.

9. CITATION:

Government of Canada
Gouvernement du Canada